AIMS Biophysics

AIMS Biophysics, 9(3): 208–220.
DOI: 10.3934/biophy.2022018
Received: 22 May 2022
Revised: 19 July 2022
Accepted: 25 July 2022
Published: 05 August 2022

http://www.aimspress.com/journal/biophysics

Research article

Molecular structure, homo-lumo analysis and vibrational spectroscopy of the cancer healing pro-drug temozolomide based on dft calculations

Ramesh Rijal[1], Hari Prasad Lamichhane[2,*] and Kiran Pudasainee[1]

[1] Physics Department, St. Xavier's College, Kathmandu, Nepal
[2] Central Department of Physics, Tribhuvan University, Kirtipur, Kathmandu, Nepal

*** Correspondence:** Email: hlamichhane1@gmail.com; Tel: +9779741695901.

Abstract: The molecular structure and spectroscopic analysis of the Temozolomide molecule have been performed using the density functional theory in neutral and anion states as well as with the addition of DMSO solvent. The 6-311G(d) basis set was employed to optimize the molecular structure of the TMZ molecule using the DFT/B3LYP method. The HOMO-LUMO energies and MEP map were computed to determine the energy gap and probable sites of electrophilic and nucleophilic reactivity in the 6-311G+(d) basis set. The vibrational frequencies were calculated using a computational method and the major fundamental modes of vibration were assigned to their respective frequencies. The potential of the computational method to explain the vibrational modes was determined by comparing simulated spectra with experimental spectra. On isotope labeling of carbon, the frequency was shifted significantly.

Keywords: DMSO; HOMO-LUMO; TMZ; MEP; isotope labeling; energy gap; vibrational spectroscopy

1. Introduction

Temozolomide, an imidazotetrazine derivative, is an oral alkylating agent synthesized at Aston University in the United Kingdom in the early 1980s [1–3]. Its molecular formula is $C_6H_5N_6O_2$ [4]. The Food and Drug Administration approved it for the treatment of glioblastoma multiforme and recurrent anaplastic astrocytoma in the first-line treatment [5,6]. All of these drugs work in a non-specific manner, affecting both malignant and non-cancerous cells [7,8]. Cancer cells, on the

other hand, divide more quickly than normal tissue, increasing vulnerability to these impacts [9]. Temozolomide, like other chemotherapy medicines, is highly costly, and drug prices might vary widely from place to place [3,10]. The mechanism of action and current clinical applicability of temozolomide has been mostly limited to glioblastoma until now [11].

Recently, computational chemistry has really drawn a lot of attention among researchers and scientists as a means of solving real problems in chemical, medicinal, biotechnology, and material science [12,13]. The main problem associated with temozolomide as a drug is its poor chemical stability in neutral and basic conditions [14]. So far, there has been no extensive theoretical research of the title compound in an anion state, and no similar studies comparing it in the presence of the solvent DMSO have been done. So, in this research paper, we optimized the temozolomide molecule at its minimum possible surface energy both in neutral and anion states and with the addition of DMSO solvent so that its frequency shifting, variation in charge distribution, and energy gap could be studied. It mainly focuses on the Mulliken charge distribution, MEP, HOMO LUMO energy gap, DOS spectrum, and vibrational spectral assignments with TED contribution in prominent peaks based on computational data compared with experimental work on previous work.

2. Methodology

All the quantum chemical calculations were performed using the Gaussian09W program [15]. The DFT/B3LYP [16,17] method and the 6-311G(d) basis set were used to generate the optimized geometrical parameters and vibrational frequencies of the molecule. Gauss View 5.0 [18] was used to perform molecular visualization and to analyze the findings. The geometry of the chosen molecule was first optimized on the potential energy surface with full relaxation at the B3LYP/6-311G (d) level and was re-optimized for subsequent calculations. The vibrational wavenumbers were then calculated using optimized structural parameters. The fact that all of the calculated wavenumbers are positive confirms the stability of optimized geometry. The DFT technique employing the same basis set has been proposed for computing the molecular electrostatic potential and electronic properties such as HOMO-LUMO energies, and DOS spectrum. According to Koopman's theorem, the energy gap is the difference between LUMO and HOMO energy [19]. The Gauss Sum program was used to observe the DOS spectrum [20]. The TED analysis was carried out using the VEDA4 program [21].

3. Results and discussion

3.1. Optimized molecular geometry

The minimum energy configuration of the temozolomide molecule is obtained by geometrical optimization of the molecule within the Gaussian 09W software. The molecular structure with its atomic numbering after optimization in a neutral state is presented in the Figure 1.

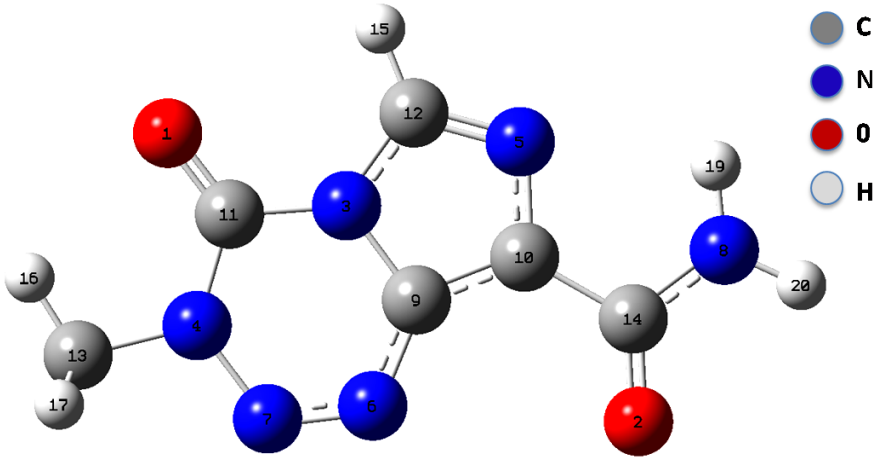

Figure 1. Optimized structure of temozolomide molecule with numbering of atoms.

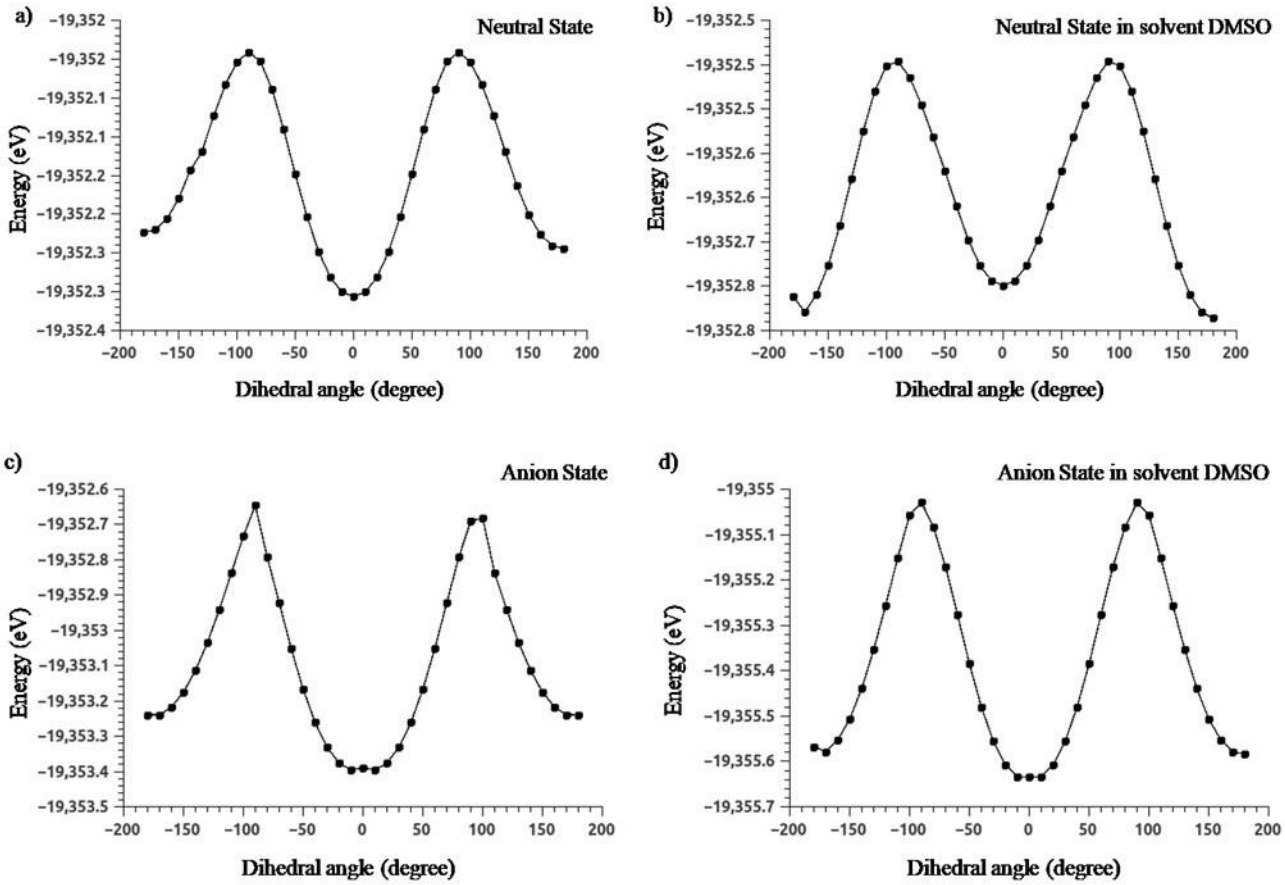

Figure 2. Potential energy surface scan of temozolomide at dihedral angle (C9–C10–C14–O2) in a) neutral state b) neutral state in DMSO solvent c) anion state and d) anion state in DMSO solvent.

Table 1. Calculated minimum total energy and their respective dihedral angles for temozolomide molecule at different states.

State	Dihedral angle (degree)	Minimum total energy (eV)
Neutral	0	-19352.31
In solvent DMSO	180	-19352.79
Anion	10	-19353.39
In solvent DMSO	0	-19355.64

The potential surface scan with the dihedral angle C9–C10–C14–O2 was performed by rotating 10 degrees in the range of 0–360 degrees for neutral and anion states. Also, the potential surface scan was performed with the addition of Dimethyl Sulfoxide (DMSO) solvent, which is shown in Figure 2, and the minimum total surface energy obtained was tabulated in Table 1. The further calculations were done by re-optimizing the molecule at its respective dihedral angles.

3.2. Molecular electrostatic potential analysis

The highest positive and negative regions, represented by blue and red colors on the MEP map, are favored sites for nucleophilic and electrophilic attacks, respectively [22]. It is very useful in the study of molecular structure and physicochemical characteristics since it uses color grading to represent positive, negative, and neutral electrostatic potential regions [23]. The temozolomide molecule has a minimum electrostatic potential primarily limited to oxygen, which is a more reactive region for an electrophilic attack. Similarly, the maximum electrostatic potential is mainly confined to hydrogen, nitrogen, and carbon, which are highly active regions for nucleophilic attack in a neutral state. However, in the anion state, almost every atom favors electrophilic attack.

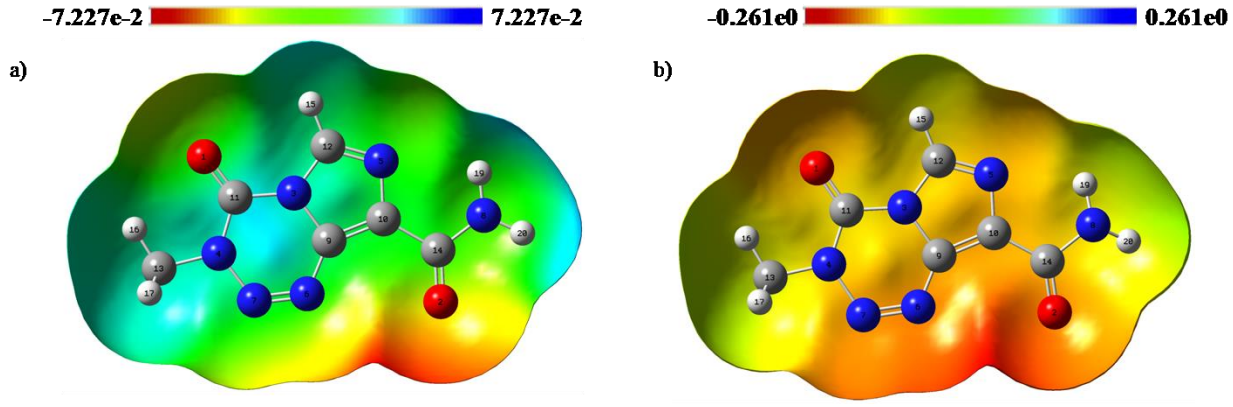

Figure 3. Molecular electrostatic potential (MEP) map of TMZ molecule in a) neutral and b) anion state.

3.3. HOMO-LUMO analysis

The frontier molecular orbitals, namely the HOMO and the LUMO have a significant role in quantum chemistry. The HOMO-LUMO orbitals of the temozolomide molecule are calculated in the

gas phase for neutral (singlet spin) and anion states (doublet spin) using the DFT method with the B3LYP/6-311G(d) basis set, as shown in Figures 4 and 5. The green and red colors represent the positive and negative phases, respectively. The energy values of HOMO (donor) and LUMO (acceptor) and their energy gaps reflect the molecule's chemical activity [24]. In general, the atom with more HOMO densities must have a higher capability to detach an electron, while the atom with higher occupied LUMO densities must have a stronger strength to gain an electron [25].

Table 2. HOMO LUMO and energy gap calculation (in eV).

Parameters	Neutral State	In solvent DMSO	Anion State	In solvent DMSO
HOMO (alpha)	-7.24	-7.15	0.52	-3.12
LUMO (alpha)	-2.84	-2.84	3.64	0.12
HOMO (beta)	**	**	-1.58	-5.16
LUMO (beta)	**	**	2.79	-0.79
Energy Gap (alpha)	4.40	4.30	3.11	3.25
Energy Gap (beta)	**	**	4.37	4.36

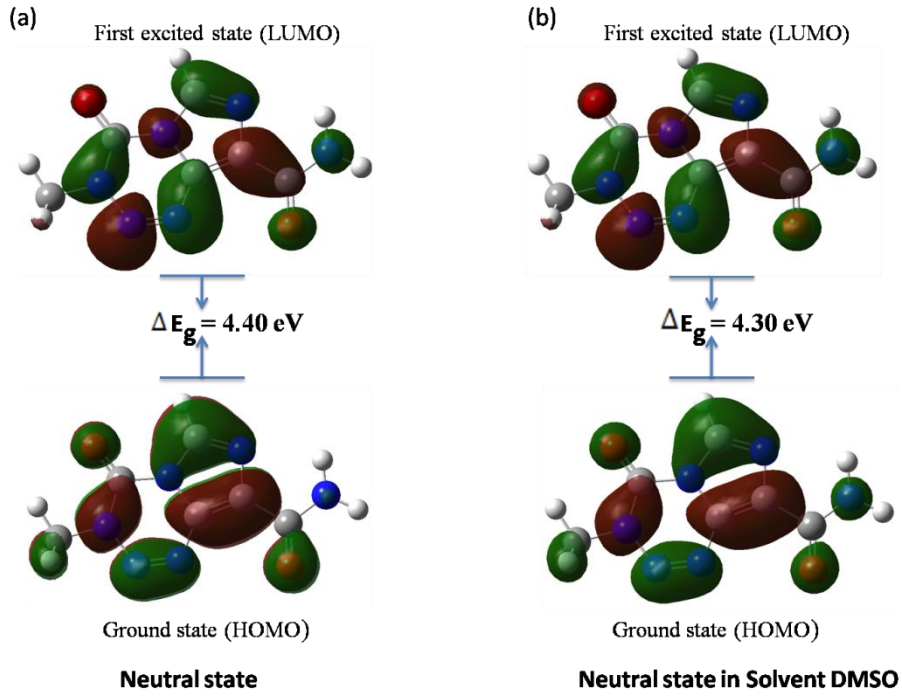

Figure 4. Frontier molecular orbitals of temozolomide molecule in a) neutral state and b) neutral state in solvent DMSO.

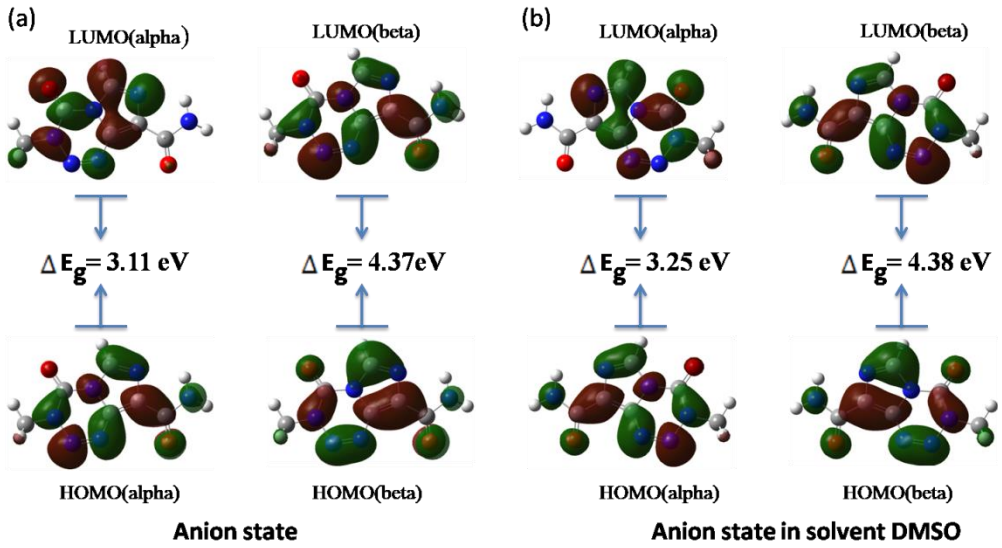

Figure 5. Frontier molecular orbitals of temozolomide molecule in a) anion state and b) anion state in solvent DMSO in doublet spin.

Table 2 lists all of the HOMO and LUMO energies, as well as their energy gaps, for different charge states of temozolomide molecule. The energy gap of the molecule in a neutral state (gas phase) is 4.40 eV and 4.30 eV when the DMSO solvent is present. Similarly, the calculated energy gaps for alpha and beta mode in anion state are found to be 3.11 eV and 4.37 eV, respectively. We have also calculated the HOMO-LUMO gap of the temozolomide molecule in water. It is found that the HOMO LUMO gaps of the title molecule in solvent water are 2.53 eV for alpha mode and 4.75 eV for beta mode respectively. The HOMO LUMO gap of the alpha mode of the title molecule is smaller in water in comparison to the molecule in DMSO. This suggests that the temozolomide molecule is more reactive in water than in DMSO. This result is consistent with previous similar work [26].

3.4. Density of states

Since the nearby orbitals in the boundary region may have quasi-degenerate energy levels, using only HOMO and LUMO to describe the frontier orbitals may not be realistic [27]. Hence, the spectrum of density of states (DOS) for the temozolomide molecule was obtained by using the Gauss Sum 3.0 program with a full width at half maximum (FWHM) of 0.3 eV [20]. The DOS spectrum explains the contribution of electrons to the conduction and valence band. The spectrum in Figures 6 and 7 illustrates how many states are available at various energy levels.

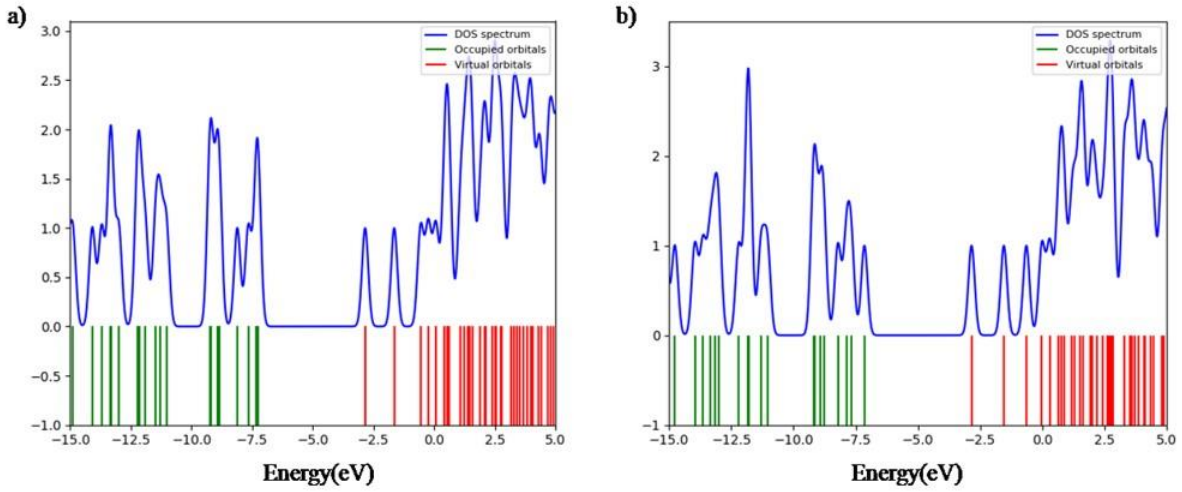

Figure 6. Density of states (DOS) spectrum of temozolomide molecule in a) neutral state and b) neutral state in solvent DMSO.

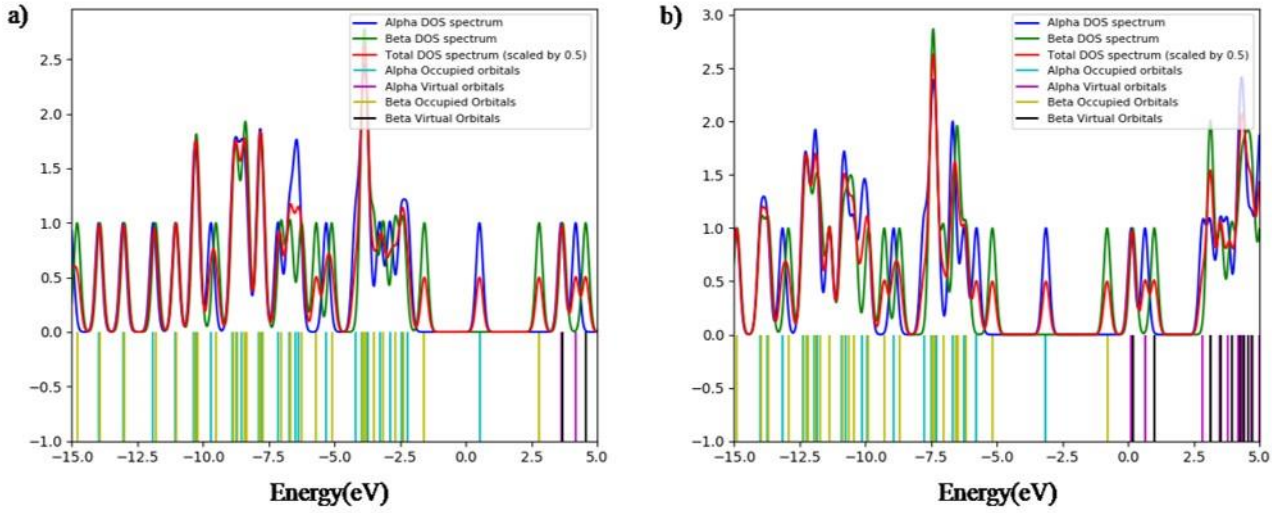

Figure 7. Density of states (DOS) spectrum (sum of alpha and beta electrons) of temozolomide molecule in a) anion state and b) anion state in solvent DMSO.

The virtual orbital is also known as an acceptor orbital because it is not occupied. The filled orbital, on the other hand, is known as the donor orbital. The DOS has a positive value for bonding interaction, a negative value for anti-bonding interaction, and is zero for no bonding interaction [28]. The energy gaps observed in the DOS spectrum and HOMO LUMO are equivalent and in good agreement with each other for both α and β-state.

3.5. Mulliken atomic charges

Mulliken atomic charge calculation is very useful in quantum chemistry since it has an influence on electronic structure, dipole moment, polarizability and various molecular properties [29].

The Mulliken atomic charges were determined in this study using the DFT/B3LYP/6-3116G+(d) basis set. The Mulliken charge values are displayed in the Figure 8. The C11 and C8 atoms have the highest positive and negative charges, respectively, both in neutral and in an anion state. Positive charges are found in all hydrogen atoms, while negative charges are found in oxygen atoms.

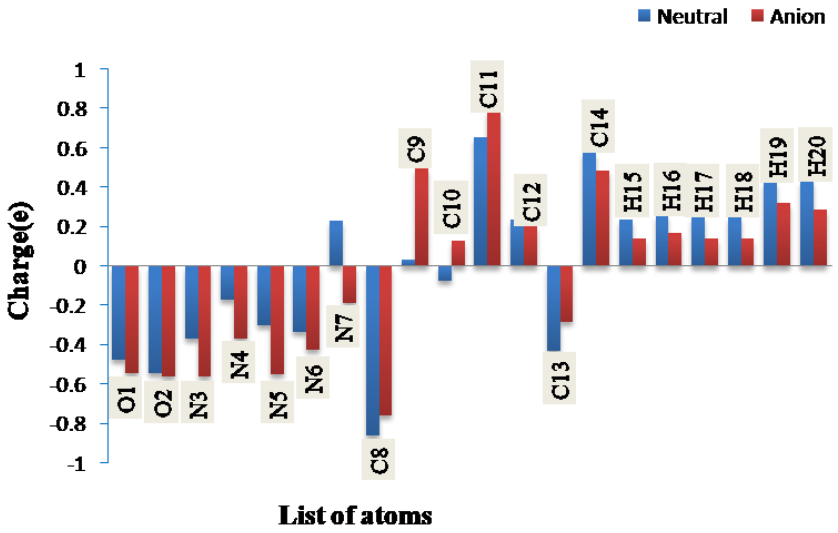

Figure 8. Mulliken charge distribution chart of the temozolomide molecule in neutral and anion state.

3.6. Vibrational analysis

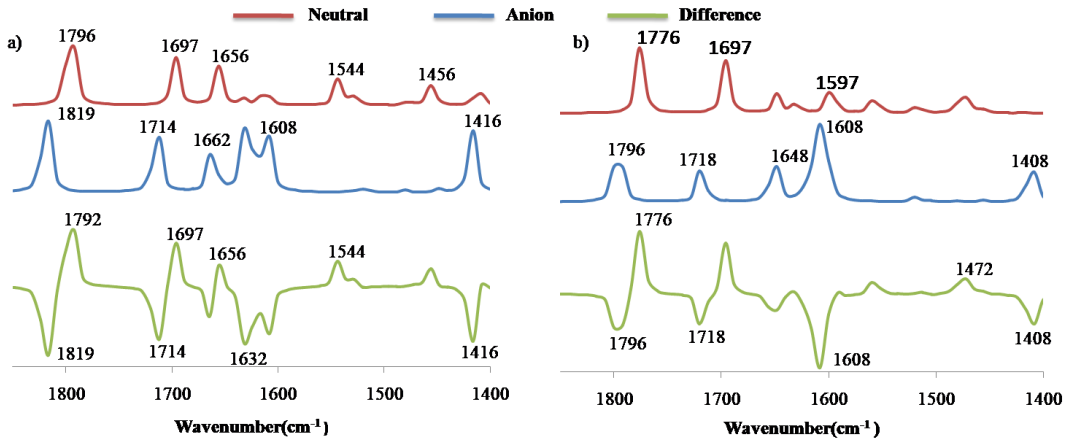

Figure 9. Calculated IR absorption spectra of neutral, anion and their difference in the frequency range of 1850–1400 cm^{-1} a) in normal mode and b) when DMSO solvent is added.

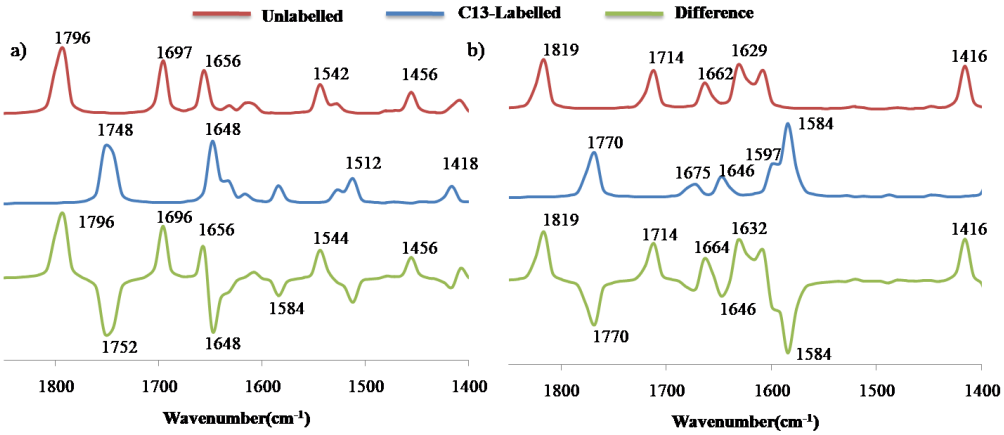

Figure 10. Calculated IR absorption spectra in the a) neutral state and b) anion state of C13-Labelled, C12-Unlabelled and their difference in the frequency range of 1850–1400 cm^{-1}.

Table 3. Calculated IR spectra with different modes of vibration and TED% in neutral and anion state.

Modes of Vibration	Frequency in normal mode (TED %)		Frequency in DMSO Solvent (TED %)	
	IR-Neutral	**IR-Anion**	**IR-Neutral**	**IR-Anion**
ν(O1-C11)	1795(78)	1819(79)	1776(77)	1796(78)
ν(N6-C9)	1632(17)	1714(20)	1630(21)	f1718(22)
δ(C9-N3-C12), δ(C10-N5-C12)	1697(13,19)	1714(16,14)	1695(11,14)	1718(20,11)
δ(H20-N8-H19)	1656(57)	1662(39)	1648(81)	1651(13)
ν(N3-C9)	1544(17)	1480(13)	1557(17)	1480(14)
δ(H15-C12-N5), ν(N5-C12)	1544(19,19)	1521(23,39)	1557(16,22)	1519(19,30)
δ(H18-C13-H17)	1529(60)	1532(60)	1520(59)	f1525(51)
τ(H17-C13-N4-C11), τ(H18-C13-N4-C11)	1529(12,12)	1532(12,12)	1520(12,13)	1525(12,12)
δ(H16-C13-H18), δ(H17-C13-H16)	1524(38,38)	1513(38,39)	1481(37,37)	1458(39,38)
τ(H16-C13-N4-C11),	1524(16)	1513(16)	1512(17)	1505(19)
ν(C14-C10)	1456(10)	1416(12)	1458(28)	1411(16)

ν= stretching, δ= bending (deformation), τ= torsion, TED= Total energy distribution

Table 4. Calculated IR spectra with different modes of vibration on isotope labeling of carbon in neutral and anion state.

Modes of Vibration	IR Frequency Neutral state		IR Frequency Anion State	
	Unlabelled	**13C-Labelled**	**Unlabelled**	**13C-Labelled**
v(O1-C11)	1796	1748	1819	1770
δ(C9-N3-C12), δ(C10-N5-C12)	1697	1648	1714	1675
δ(H20-N8-H19)	1656	1635	1662	1646
v(N6-C9)	1632	1615	1629	1597
v(N3-C9), δ(H15-C12-N5)	1542	1528	1530	1531
v(C14-C10)	1456	1418	1416	1390

v= stretching, δ= bending (deformation)

The title molecule is made up of 20 atoms and consists of 54 different vibrational modes. The intensive vibrational modes occurring between 1850 and 1400 cm^{-1} were observed and analyzed with their TED assignment for the neutral and anion state of the compound. Also, the vibrational shifts were observed in addition of the DMSO solvent and isotope labeling of carbon atoms.

The most prominent peak for the title molecule in the selected range was observed at 1819 cm^{-1} with TED contribution of 79% maximum in anion state. It is due to the stretching mode of C=0 which are usually observed in the region of 1850-1650 cm^{-1} [30]. Usually, the ring C-C aromatic vibrations observed in the IR cover the spectral range from 1600 to 1400 cm^{-1} [31]. In our study, the C-C stretching vibration bands with their TED assignments are calculated at 1456 (10), 1416 (12), 1458 (28), and 1411 (16) cm^{-1} in the IR spectrum of neutral, anion, and in the presence of DMSO solvent for both states, respectively.

The stretching vibration of C-N is commonly found around 1400 cm^{-1} [31]. The computed wavenumbers for C-N vibration are observed between 1700 cm^{-1} and 1520 cm^{-1} in neutral and anion states, as well as in the presence of solvent and isotope labeling of carbon atoms. The calculated value slightly differs since it is not scaled and resonance in the ring increases the force constant of the C-N bond [32].

When an atom is replaced by an isotope of larger mass, a downshift in the frequency can be observed [33]. The frequency of every mode of vibration between 1850 and 1400 cm^{-1} has decreased slightly when the carbon atom was labeled with the C-13 isotope in neutral and anion states. In an average, the down shifting ranges from 20-80 cm^{-1} which is remarkably noticeable in the Figures 9 and 10.

4. Conclusions

The minimum stable energy for the potential surface scan was found in the anion state and in the presence of DMSO solvent. The nucleophilic and electrophilic reaction sites of the molecule are predicted by the MEP surface. The Mulliken atomic charges were examined and analyzed. The

HOMO and LUMO energy gaps address every charge transfer interaction that occurs within the molecule and its bioactivity. The more value of the HOMO-LUMO gap in the neutral state of the temozolomide molecule reflects the higher kinetic stability and the lower chemical reactivity both in the gas phase and in solvents. The energy gaps observed in the DOS spectrum and HOMO-LUMO are equivalent and correspond well with each other. Also, the vibrational frequencies with their corresponding frequencies are analyzed both in the gas phase and in the presence of DMSO solvent. The calculated frequencies of all modes of vibration are present within the characteristic region of the spectrum, and the frequency shifting was observed significantly in different charge states and isotope labeling of carbon.

Acknowledgements

We are very thankful to the University Grant Commission of Nepal for providing financial support and to St. Xavier's College for providing computational support.

Conflict of interest

All authors declare no conflicts of interest in this paper.

References

1. Newlands ES, Stevens MFG, Wedge SR, et al. (1997) Temozolomide: a review of its discovery, chemical properties, pre-clinical development and clinical trials. *Cancer Treat Rev* 23: 35–61. https://doi.org/10.1016/S0305-7372(97)90019-0
2. Svec RL, McKee SA, Berry MR, et al. (2022) Novel imidazotetrazine evades known resistance mechanisms and is effective against temozolomide-resistant brain cancer in cell culture. *ACS Chem Bio l* 17: 299–313. https://doi.org/10.1021/acschembio.2c00022
3. Wesolowski JR, Rajdev P, Mukherji SK (2010) Temozolomide (Temodar). *Am J Neuroradiol* 31: 1383–1384. https://doi.org/10.3174/ajnr.A2170
4. National Center for Biotechnology Information: PubChem Compound Summary for CID 11830328, Temozolomide Acid, 2022. Available from: https://pubchem.ncbi.nlm.nih.gov/compound/Temozolomide-Acid.
5. VillanoJL, SeeryTE, BresslerLR (2009) Temozolomide in malignant gliomas: current use and future targets. *Cancer Chemoth Pharm* 64: 647–655. https://doi.org/10.1007/s00280-009-1050-5
6. Sansom C (1999) Temozolomide presents breakthrough in glioblastoma multiforme treatment. *Pharm Sci Technol Toda y* 4: 131–133.
7. Louis DN, Perry A, Reifenberger G, et al. (2016) The 2016 World Health Organization classification of tumors of the central nervous system: a summary. *Acta Neuropathol* 131: 803–820. https://doi.org/10.1007/s00401-016-1545-1
8. O'reilly SM, Newlands ES, Brampton M, et al. (1993) Temozolomide: A new oral cytotoxic chemotherapeutic agent with promising activity against primary brain tumours. *Eur J Cancer* 29: 940–942. https://doi.org/10.1016/S0959-8049(05)80198-4

9. Bower M, Newlands ES, Bleehen NM, et al. (1997) Multicentre CRC phase II trial of temozolomide in recurrent or progressive high-grade glioma. *Cancer Chemoth Pharm* 40: 484–488. https://doi.org/10.1007/s002800050691
10. Klepper B, Pauker D (2006) Medicare's drug plan: huge price disparities for common cancer drugs. *Community Oncol* 12: 753–755. https://doi.org/10.1016/S1548-5315(11)70942-1
11. Thomas A, Tanaka M, Trepel J, et al. (2017) Temozolomide in the era of precision medicine. *Cancer Res* 77: 823–826. https://doi.org/10.1158/0008-5472.CAN-16-2983
12. Kumer A, Sarker MN, Paul S (2019) The thermo physical, HOMO, LUMO, vibrational spectroscopy and QSAR study of morphonium formate and acetate ionic liquid salts using computational method. *Turk Comput Theor Chem* 3: 59–68. https://doi.org/10.33435/tcandtc.481878
13. Kumer A, Paul S, Sarker M, et al. (2019) The prediction of thermo physical, vibrational spectroscopy, chemical reactivity, biological properties of morpholinium borate, phosphate, chloride and bromide ionic liquid: a DFT study. *Int J New Chem* 6: 236–253. https://doi.org/10.22034/ijnc.2019.110412.1053
14. Yahiaoui K, Seridi L, Mansouri K (2021) Temozolomide binding to Cucurbit[7]uril: QTAIM, NCI-RDG and NBO analyses. *J Incl Phenom Macro Chem* 99: 61–77. https://doi.org/10.1007/s10847-020-01027-5
15. Frisch MJ, Trucks GW, Schlegel HB, et al. (2009). Gaussian 09 Package. Gaussian. Inc., Wallingford, CT.
16. Becke A (1993) Density-functional thermochemistry.III. The role of exact exchange. *J Chem Phys* 98: 5648–5652. https://doi.org/10.1063/1.464913
17. Lee C, Yang W, Parr RG (1998) Development of the Colle-Salvetti correlation-energy formula into a functional of the electron density. *Phys Rev B* 37: 785–789. https://doi.org/10.1103/PhysRevB.37.785
18. Dennington R, Keith T, Millam J (2009) GaussView, Version 5.0. 8, R. Dennington: Semichem Inc.
19. Koopmans T (1934) Über die zuordnung von wellenfunktionen und eigenwerten zu den einzelnen elektronen eines atoms. *Physica* 1: 104–113. https://doi.org/10.1016/S0031-8914(34)90011-2
20. O'boyle NM, Tenderholt AL, Langner KM (2008) A library for package-independent computational chemistry algorithms. *J Comput Chem* 29: 839–845. https://doi.org/10.1002/jcc.20823
21. Jamróz MH (2013) Vibrational energy distribution analysis (VEDA): scopes and limitations. *Spectrochim Acta A Mol Biomol Spectrosc* 114: 220–230. https://doi.org/10.1016/j.saa.2013.05.096
22. Nkungli NK, Ghogomu JN (2017) Theoretical analysis of the binding of iron (III) protoporphyrin IX to 4-methoxyacetophenone thiosemicarbazone via DFT-D3, MEP, QTAIM, NCI, ELF, and LOL studies. *J Mol Model* 23: 200. https://doi.org/10.1007/s00894-017-3370-4
23. Krack M, Jug K (1996) Molecular electrostatic potentials for large systems, In: Murray, J.S., Kalidas, S., *Theoretical and Computational Chemistry*, Amsterdam: Elsevier, 297–331. https://doi.org/10.1016/S1380-7323(96)80047-1

24. Gunasekaran S, Balaji RA, Kumaresan S, et al. (2008) Experimental and theoretical investigations of spectroscopic properties of N-acetyl-5-methoxytryptamine. *Can J Anal Sci Spectrosc* 53: 149–162.
25. Kumar PS, Vasudevan K, Prakasam A, et al. (2010) Quantum chemistry calculations of 3-Phenoxyphthalonitrile dye sensitizer for solar cells. *Spectrochim Acta A Mol Biomol Spectrosc* 77: 45–50. https://doi.org/10.1016/j.saa.2010.04.021.
26. Sang-Aroon W, Ruangpornvisuti V, Amornkitbamrung V (2016) Tautomeric transformation of temozolomide, their proton affinities and chemical reactivities: a theoretical approach. *J Mol Graph Model* 66: 76–84. https://doi.org/10.1016/j.jmgm.2016.03.016
27. AlRabiah H, Muthu S, Al-Omary F, et al. (2017) Molecular structure, vibrational spectra, NBO, Fukui function, HOMO-LUMO analysis and molecular docking study of 6-[(2-methylphenyl)sulfanyl]-5-propylpyrimidine-2,4(1H,3H)-dione. *Maced J Chem Chem Eng* 36: 59–80. https://doi.org/10.20450/mjcce.2017.1001
28. Chen M, Waghmare UV, Friend CM, et al. (1998) A density functional study of clean and hydrogen-covered α-MoO3 (010): Electronic structure and surface relaxation. *J Chem Phys* 109: 6854–6860. https://doi.org/10.1063/1.477252
29. Mulliken RS (1955) Electronic population analysis on LCAO–MO molecular wave functions. *J Chem Phys* 23: 1833–1840. https://doi.org/10.1063/1.1740588
30. Socrates G (2004) *Infrared and Raman Characteristic Group Frequencies: Tables and Charts*, 3 Eds., Chichester: John Wiley and Sons Ltd, 12–14.
31. Sui H, Ju X, Liu X, et al. (2014) Primary thermal degradation effects on the polyurethane film. *Polym Degrad Stabil* 101: 109–113. https://doi.org/10.1016/j.polymdegradstab.2013.11.021
32. Wolpert M, Hellwig P (2006) Infrared spectra and molar absorption coefficients of the 20 alpha amino acids in aqueous solutions in the spectral range from 1800 to 500 cm^{-1}. *Spectrochim Acta A Mol Biomol Spectrosc* 64: 987–1001. https://doi.org/10.1016/j.saa.2005.08.025
33. Tanskanen H, Khriachtchev L, Lundell J, et al. (2004) Organo-noble-gas hydride compounds HKrCCH, HXeCCH, HXeCC, and HXeCCXeH: Formation mechanisms and effect of 13 C isotope substitution on the vibrational properties. *J Chem Phys* 121: 8291–8298. https://doi.org/10.1063/1.1799611

AIMS Press